Characterization of Nanofibrillated Cellulose Produced From Oil Palm Empty Fruit Bunch Fibers (OPEFB) Using Ultrasound

R. Rosazley [1]*, M.Z. Shazana [1], M.A. Izzati [1], A.W. Fareezal [1], I. Rushdan [2] and Z.M.A. Ainun [3]
[1] Department of Physics, Faculty of Science and Mathematics,
Universiti Pendidikan Sultan Idris,
35900 Tanjong Malim, Perak, Malaysia.
[2] Forest Research Institute Malaysia (FRIM), 52109 Kepong, Selangor, Malaysia.
[3] Laboratory of Biopolymer and Derivatives, Institute of Tropical Forestry and Forest Products (INTROP), Universiti Putra Malaysia, 43400 UPM Serdang, Selangor, Malaysia.
*E-mail: rosazley@fsmt.upsi.edu.my

Abstract

Characterization of nanofibrillated cellulose (NFC) from oil palm empty fruit bunches (OPEFB) using ultrasound has been investigated. Cellulose from OPEFB pulp was gained by soda-anthraquinone (AQ) pulping and bleaching processes. The ultrasound with 20 kHz frequencies and 700 W output power was used in order to produce the NFC. Results were assessed by using fourier-transform infrared spectroscopy (FTIR) for structural analysis. The thermal stabilities were analyzed using thermogravimetric analysis (TGA) and crystalline index was measured using X-ray diffraction (XRD). Meanwhile, the morphology structure was carried out by field emission scanning electron microscope (FE-SEM) and scanning transmission electron microscopy (STEM). The diameters of the OPEFB-NFC were obtained between 5 to 23 nm. The FTIR results showed that removal of lignin, hemicelluloses and waxes after bleaching process. The TGA and XRD analysis showed that OPEFB-NFC had higher thermal stability and crystallinity as compared to OPEFB-Pulp and OPEFB-Cellulose. Finally, it is demonstrated that OPEFB-NFC has good potential in vast application especially for reinforced composite materials.

Keywords Nanofibrillated cellulose, Oil palm empty fruit bunch fibers, Ultrasound

1. Introduction

Malaysia is listed as one of the largest producers and exporters of palm oil in the world. It has been reported that 4.49 million hectares of land covered in Malaysia is under oil palm cultivation, accounts 39 % of world palm oil production and for world exports is 44 % (Rosnah et. al., 2004). One tone of palm can generate approximately 20 % oil and 80 % biomass (Osman et al, 2013). Malaysia alone can produce around 40 million tons of oil palm biomass per year and in terms of empty fruits bunches the total capacity is 280,000 tones. This oil palm empty fruit bunch (OPEFB) can be categorized as lignocellulosic agricultural waste and causes undesirable environmental impacts (Chiew et al., 2013; Ireana et al., 2014). The chemical composition of OPEFB consists of 44.4% cellulose, 30.9% hemicelluloses and 14.2% lignin. The high cellulose and low lignin content condition provides vast potential resources to value-added products. This is due to cellulosic biomass are inexhaustible, renewable, biodegradable, recyclable and also derivatizable biopolymer (Ferrer et al., 2012; Nazir et al., 2013).

The terminology nanofibrillated cellulose (NFC) is applied which the fibrils diameter is measured less than 100 nm and several micrometers in length (Zimmerman et al., 2010; Lin et. al., 2014). NFC also consists of long, flexible, entangled cellulose nanofibers, alternating crystalline and amorphous domains (Kalia et al., 2014). Research in nano-size cellulose has

attracted the interest of various parties because of its properties. Among the interesting properties in utilizing nano-size cellulose are high specific strength and stiffness, high aspect ratio, large specific surface area, high reinforcing potential and low weight (Li et al., 2012; Ghaderi et al., 2014). Thus, its unique features have gained high attention in wide range applications such as polymeric nanocomposite (Eita et al., 2011; Hu et al., 2014), packaging and food packaging (Ghaderi et al., 2014), reinforce materials (Pasquini et al., 2010), printing paper (Ghazali et al., 2014), antibacterial paper (Martins et al., 2013) and conductive nanopaper (Salajkova et al., 2013).

Ultrasonication using oscillating power to isolate micro-size cellulose fibrils into nano-size fibers by hydrodynamics forces of ultrasound. During ultrasonication, the phenomena called acoustic cavitation which refers to the formation, growth and implosive collapse of bubbles in liquid cause hot spots due to powerful mechanical oscillating power and high intensive waves. Cavitations process supplies around 10-100 kJ/mol energy and this energy is actually within the hydrogen bond energy scale (Tischer et. al, 2010). Consequently, NFC which is a combination of micro-sized fibers and nano- sized fibrils with web-like structures can be formed (Rezanezhad et al., 2013; Kangas et al., 2014).

2. Materials and Methods

Oil palm empty fruit bunch (OPEFB) fibers as a starting material of cellulose were supplied by Forest Research Institute Malaysia (FRIM). Meanwhile, sodium hydroxide, chlorine dioxide, acetic acid and anthraquinone (AQ) were purchased from Merck and Co. Inc. The pulp was produced by using soda-anthraquinone pulping technique and carried out in a rotary digester. Pulping reaction time was divided into two stages which acquired 60 min in stage one and 90 min in stage two. The reaction temperature for both stages was 170 °C. Then, pre-hydrolysis process was carried out for 60 min. After washing process, the pulp was filtered and stored at 5 °C until further use. Cellulose was obtained by using seven stages bleaching processes using chlorine dioxide, acetic acid and sodium hydroxide. The consistency was retained at 10 %. Then, the time was varied from 60 to 120 min and the temperature condition was maintained at 70 °C. Table 1 shows the detail conditions of bleaching processes for OPEFB pulp. A 5 g (oven dry) of cellulose was dispersed in 500 ml of distilled water using mechanical stirrer. After that, 20 kHz sonication probe with a 700 W output power, model Q-Sonica 700 manufactured by Qsonica, LLC, USA was used to produce NFC. The total time of ultrasonic treatment was 60 min and was performed in room temperature. Microstructural analysis was characterized using a field emission scanning electron microscope (FE-SEM) and scanning transmission electron microscope (STEM) (Hitachi, Japan). Meanwhile, fourier transform infrared instrument (FTIR) spectra was recorded using Nicolet 6700 (Thermo Scientific, USA). Thermogravimetric analysis (TGA) was performed using Pyris 1 TGA (Perkin Elmer, USA) instrument. The temperature was run from 30 to 550 ^{O}C at a heating rate of 10 ^{O}C/min and nitrogen gas flow rate of 20 ml/min. X-ray diffraction (XRD) measurements were performed on a D8 Advance (Bruker AXS, Germany) using Cu Kα radiation at 40 kV and 40 mA. The samples were scanned over a 2θ range varying from 10^{O} to 70^{O}. The crystallinity index of samples was calculated as crytallinity = ($I_{cry} - I_{am}$ / I_{cry}) x 100, where I_{cry} represents the crystalline part of the sample. Meanwhile, I_{am} is represents the amorphous part.

3. Results and Discussion

3.1 Morphology of the Treated and Untreated OPEFB Fibers

Fig. 1 shows the morphology structure of OPEFB-Cellulose before and after ultrasonication treatment by using FE-SEM and STEM microscope. It was observed that before ultrasonication treatment the cellulose from soda-anthraquinone pulping and bleached fibers exhibited smooth and clear surfaces due to the removal of the impurities as shown in Fig. 1a. Meanwhile, after the ultrasonication treatment, as can be seen clearly that shows external fibrillation on the surfaces (Fig. 1b). It can be explained by cavitation impacts, which are formation, growth and implosive collapse of bubbles in liquid cause hot spots due to powerful mechanical oscillating power and high intensive waves. Actually, when lower frequency ultrasonic was used the bubbles that formed become larger, which was implode releasing greater energy. However, the thickness of the barrier layer was reduced. Eventually, the oscillating power isolated micro-size cellulose fibrils into nano-size fibers with web- like structures by hydrodynamics forces of ultrasound as shown in Fig. 1c. In this study, the diameters of the OPEFB-NFC were obtained between 5 to 23 nm.

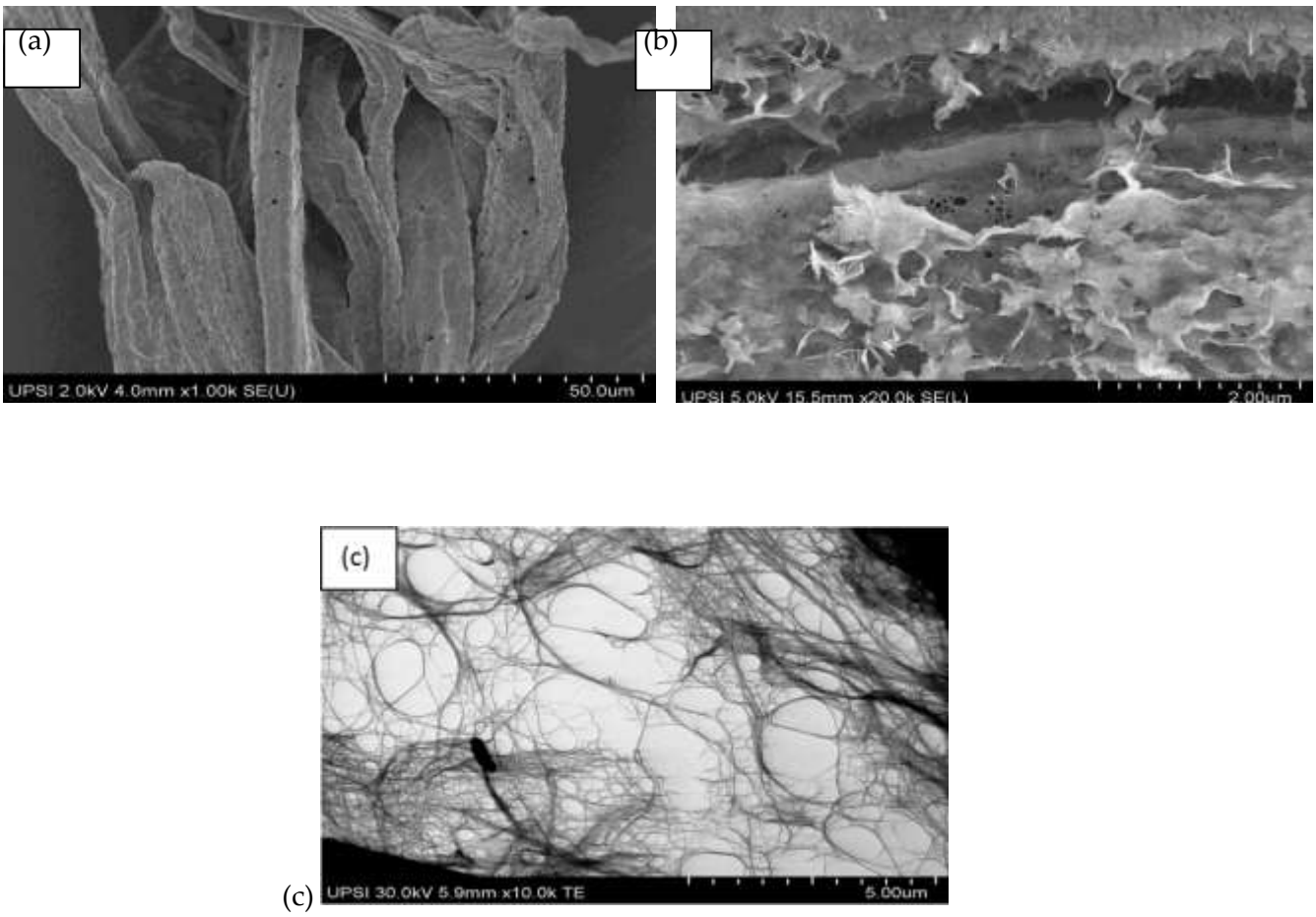

Figure 1 FE-SEM micrographs of cellulose (a) OPEFB before ultrasonic treatment; (b) OPEFB after ultrasonic treatment. Meanwhile, STEM micrograph of cellulose (c) OPEFB after ultrasonic treatment

3.2 X-RAY Diffraction Analysis (XRD)

Fig. 2 shows an XRD diffractogram of the OPEFB-Pulp, OPEFB-Cellulose and OPEFB-NFC. It was obviously seen that two peaks around $2\theta = 15^{o}$ and 22.6^{o} represents the amorphous and crystalline region, respectively. It was also proved the typical cellulose I structure present (Haafiz et al. 2013; Ireana et al. 2014). The X-ray diffraction patterns obtained shown similarity, indicating maintenance of cellulose structure after ultrasonication process. It can be seen, the intensity of OPEFB- NFC becomes higher as compared to OPEFB-Cellulose and OPEFB-Pulp. This is due to the degradation or removal of hemicelluloses, lignin and waxy materials in amorphous region by ultrasonication process, which is the crystallinity of OPEFB-NFC (70.50%), followed by OPEFB- Cellulose (58.26%) and OPEFB-Pulp (52.74%) as shown in Fig. 3 (Haafiz et al., 2013; Ireana et al., 2014).

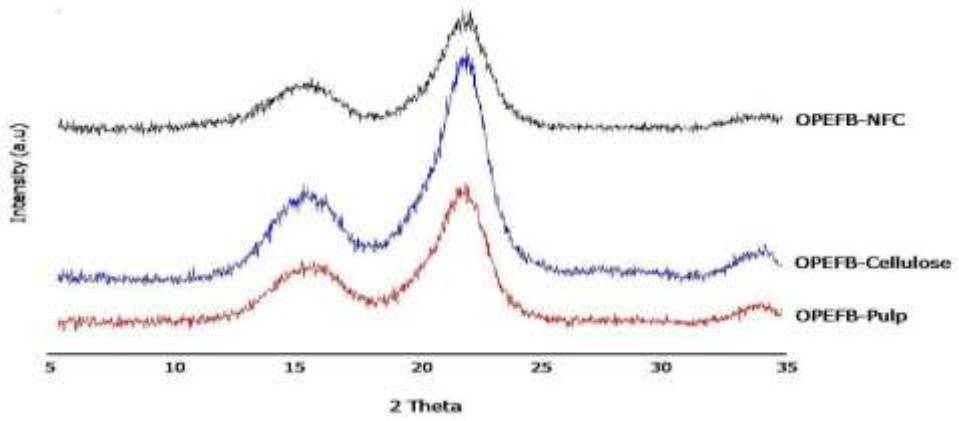

Figure 2 X-ray diffractograms of OPEFB-Pulp, OPEFB-Cellulose and OPEFB-NFC with ultrasonic treatment at 20 kHz and 700 W for 60 min

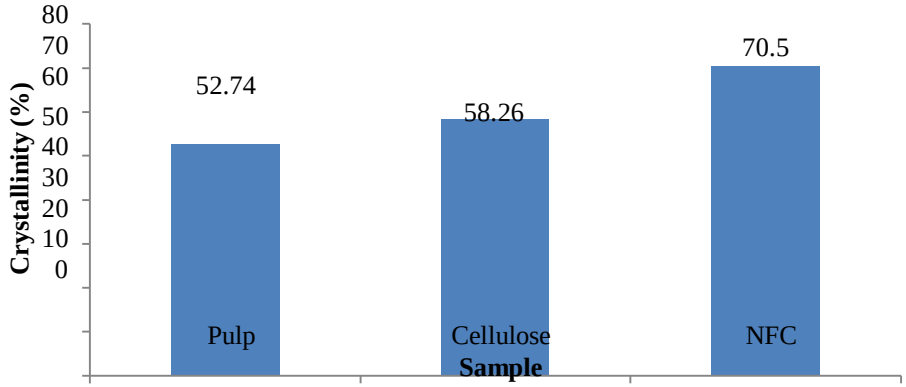

Figure 3 The percentage of crystallinity of OPEFB-Pulp, OPEFB-Cellulose and OPEFB-NFC with ultrasonic treatment at 20 kHz and 700 W for 60 min

3.3 FTIR Analysis

Fig. 4 shows the FTIR spectra of the OPEFB-Pulp, OPEFB-Cellulose and OPEFB-NFC. As can be seen, the spectra obtained shows that absorption bands at 3349 cm^{-1} represent the stretching vibration of O-H. This stretching exist was due to moisture content where in lignin, hemicelluloses and cellulose present the hydroxyl groups (Ireana et al., 2014). The C-H stretching vibration in cellulose, hemicelluloses and lignin was identified in the spectrum at 2900 cm^{-1}. The transmittance peak at 1645 cm^{-1} was observed attributed to the O-H bending vibration due to water absorption and related to the bending modes of water molecules from strong interaction between cellulose and water (Nazir et al., 2013; Haafiz et al., 2013). Actually, there is no penetration of water at the crystalline cellulose. However, dry amorphous cellulose can absorb water and become soft and flexible (Xing et al. 2010).

The peak intensity at 1462 cm^{-1} present in the spectrum was attributed to the symmetric bending of CH_2. Meanwhile, the absorption peak at 1313 cm^{-1} was due to existence of bending vibration from C-H and C-O bonds in the polysaccharide aromatic rings of cellulose (Ireana et al., 2014). The peaks at 1216 cm^{-1} and 1157 cm^{-1} were attributed to C-O-C of arylalkyl ether in lignin and C-H rocking vibration, respectively. The spectrum showed the peak at 1047 cm^{-1} due to characteristic of anhydroglucose chains with a C-O stretch. Then, the peak at 898 cm^{-1} corresponds to C-H glycosidic deformation or β-gycosidic linkage and also known as the amorphous band (Nazir et al., 2013; Ireana et al., 2014).

The spectrum also shows the absence of peaks range 1509 to 1609 cm^{-1} and 1700 to 1740 cm^{-1}. This is representing C=C aromatic skeletal vibrations and either the acetyl or ester groups of hemicellulose, which is indicate that all the lignin was removed and removal of hemicellulose. Eventually, the mechanical treatment by ultrasonication process of OPEFB-Pulp did not affect the cellulosic components of OPEFB NFC.

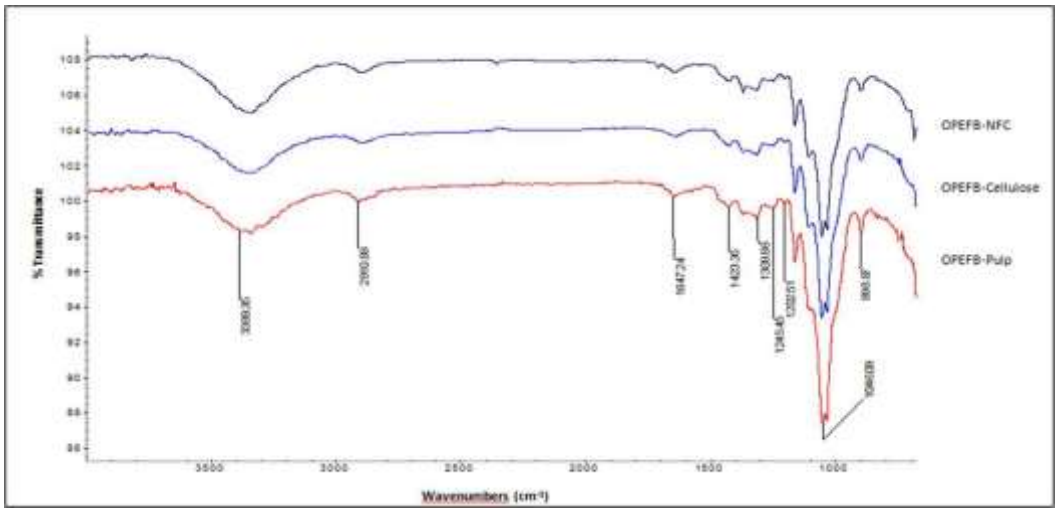

Figure 4 FTIR spectra of OPEFB-Pulp, OPEFB-Cellulose and OPEFB-NFC with ultrasonic treatment at 20 kHz and 700 W for 60 min

3.4 Thermogravimetric Analysis (TGA)

Fig. 5 shows the TGA curves that represent the thermal decomposition of OPEFB-Pulp, OPEFB-Cellulose and OPEFB-NFC. All samples showed the same pattern of degradation. It can be seen, all samples initiated to decompose at 30 ^{O}C. These phenomena attributed to the evaporation of absorbed water in the fibers and nanofibers (Li et al., 2012; Ireana et al., 2014). The rapid decomposition of OPEFB-NFC occurred at 361 to 410 ^{O}C. Meanwhile, the OPEFB-Pulp and OPEFB-Cellulose decompose rapidly at 361 to 410 ^{O}C and 361 to 410 ^{O}C, respectively. It was analyzed that OPEFB-NFC had the highest thermal stability. The pattern of degradation can be explained by the hemicelluloses begin to decompose below 400 ^{O}C. Then, the pyrolysis of lignin happened and followed by depolymerization of cellulose. Finally, active flaming combustion and char oxidation occurred on samples (Haafiz et al., 2013). The results obtained shows that the crystallinity and value of DP were considered as factors influenced the thermal stability of the samples (Rezanezhad et al., 2013).

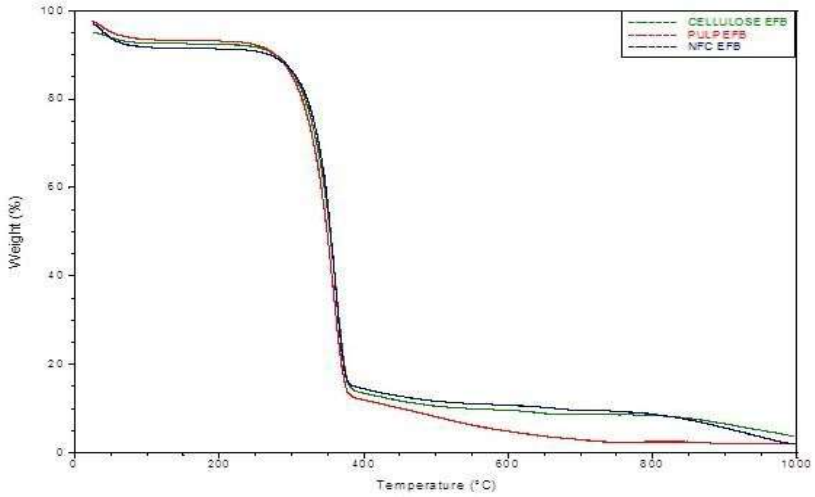

Figure 5 TGA thermograms of OPEFB-Pulp, OPEFB-Cellulose and OPEFB-NFC with ultrasonic treatment at 20 kHz and 700 W for 60 min

4. Conclusion

Nanofibrillated cellulose (NFC) was successfully prepared from oil palm empty fruit bunch fibers (OPEFB) via ultrasound-assisted at 20 kHz frequency and output power of 700 W. The NFC had diameters between 4 to 23 nm. In terms of thermal stability the OPEFB-NFC showed high value as compared to OPEFB-Pulp and OPEFB-Cellulose. Meanwhile, the viscosity and degree of polymerization of OPEFB-NFC showed deteriorate pattern which is OPEFB-NFC<OPEFB-Cellulose<OPEFB-Pulp.

Acknowledgements

We acknowledge the financial support from Universiti Pendidikan Sultan Idris (UPSI) for the short- term grant (Code: 2012-0068-102-01 and 2015-0047-102-01) and Ministry of Higher Education for the Program Research Acculturation Collaborative Effort (RACE) grant (Code: 2012-0148-102-62).

References

M.S. Rosnah, A.G.M. Top, W.H.W. Hassan. (2004). Production of carboxymethycellulose (CMC) from oil palm empty fruit bunch (EFB), MPOB Information Series, 228.

H. Osman, T.P. Ling, M.Y. Maskat, R.M. Illias, K. Badri, J. Jahim, N.M. Mahadi. (2013). Optimization of pretreatments for the hydrolysis of oil palm empty fruit bunch fiber (EFBF) using enzyme mixtures, *Biomas and Bioenergy*. 56, 137-146.

Y.L. Chiew, S. Shimada. (2013). Current state and environmental impact assessment for utilizing oil palm empty fruit bunches for fuel, fiber and fertilizer – a case study of Malaysia, *Biomass and Bioenergy*. 51. 109-124.

A.F. Ireana Yusra, H.P.S. Abdul Khalil, M.S. Hossain, A.A. Astimar, Y. Davoudpour, R. Dungani, A. Bhat. (2014). Exploration of a chemo-mechanical technique for the isolation of nanofibrillated cellulosic fiber from oil palm empty fruit bunch as a reinforcing agent in composites materials, *Polymers*. 6, 2611-2624.

A. Ferrer, I. Filpponen, A. Rodríguez, J. Laine, O.J. Rojas. (2012). Valorization of residual empty palm fruit bunch fibers (EPFBF) by microfluidization: Production of nanofibrillated cellulose and EPFBF nanopaper, *Bioresour. Technol*. 125, 249-255.

M.S. Nazir, B.A. Wahjoedi, A.W. Yussof, M.A. Abdullah. (2013). Eco-friendly extraction and characterization of cellulose from oil palm empty fruit bunches, *Bioresource*. 8(2), 2161-2172.

T. Zimmermann, N. Bordeanu, E. Strub. (2010). Properties of nanofibrillated cellulose from raw materials and its reinforcement potential, *Carbohyd.Polym.* 79(4), 1086-1093.

J. Lin, L. Yu, F. Tian, N. Zhao, X. Li, F. Bian, J. Wang. (2014). Cellulose nanofibrils aerogels generated from jute fibers, *Carbohyd.Polym.* 109, 35-43.

S. Kalia, S. Boufi, A. Celli, S. Kango. (2014). Nanofibrillated cellulose: surface modification and potential applications, *Colloid Polym. Sci*. 292, 5-31.

W. Li, J. Yue, S. Liu. (2012). Preparation of nanocrystalline cellulose via ultrasound and its reinforcement capability for poly(vinyl alcohol) composites, *Ultrasonic Sonochemistry*. 19(3), 479-485.

M. Ghaderi, M. Mousavi, H. Yousefi, M. Labbafi. (2014). All-cellulose nanocomposite film made from bagasse cellulose nanofibers for good packaging application, *Carbohyd.Polym.* 104, 59-65.

M. Eita, H. Arwin, H. Granberg, L. Wågberg. (2011). Addition of silica nanoparticles to tailor the mechanical properties of nanofibrillated cellulose thin films, *Journal of Colloid and Interface Science.* 363(2), 566-572.

K. Hu, D.D. Kulkarni, I. Choi, V.V. Tsukruk. (2014). Graphene-polymer nanocomposites for structural and functional applications, *Progress in Polymer Science*. 39(11), 1934-1972.

A. Ghazali, Y.M. Dermawan, M.R.H.M. Zukeri, R. Ibrahim, S. Ghazali. (2014). EFB nano fibrous cells for paper smoothing and improved printability, *Advanced Materials Research.* 832, 537-542.

M. Salajkova, L. Valentini, Q. Zhou, L.A. Berglund. (2013). Tough nanopaper structures based on cellulose nanofibers and carbon nanotubes, *Composites Science and Technology*. 87, 103-110.

M. Xing, S. Yao, S.K. Zhou, Q. Zhao, J.H. Lin, J.W. Pu. (2010). The influence of ultrasonic treatment on the bleaching of cmp revealed by surface and chemical structural analyses, *Bioresource.* 5(3), 1353-1365.

P.C.S.F. Tischer, M.R. Sierakowski, H. Westfahl, C.A. Tischer. (2010). Nanostructural reorganization of bacterial cellulose by ultrasonic treatment, *Biomacromolecules.* 11(5), 1217-1224.

S. Rezanezhad, N. Rezanezhad, G. Asadpur. (2013). Isolation of nanocellulose from waste via ultrasonication, *Lignocellulose.* 2(1), 282-291.

H. Kangas, P. Lahtinen, A. Sneck, A.M. Saariaho, O. Laitinen, E. Hellén. (2014). Characterization of fibrillated cellulose. A short review and evaluation of characteristics with a combination of methods, *Nordic Pulp & paper Research Journal*. 29(1), 129-143.

M.K.M. Haafiz, S.J. Eichhorn, A. Hassan, M. Jawaid. (2013). Isolation and characterization of microcrystalline cellulose from oil palm biomass residue, *Carbohyd.Polym*. 93(2), 628-634.